Experimental demonstration of the proportionality of RF reception field to $\mathbf{B}_1^{-*}$ in a complex vector space

Hidehiro Watanabe[1]

[1]*Center for Environmental Measurement and Analysis, National Institute for Environmental Studies, Tsukuba, Ibaraki, Japan*

Introduction

High field MRI with a feature of high sensitivity and contrast can provide highly resolved images and spectra. However, image non-uniformity occurs due to RF inhomogeneous distribution inside a dielectric sample such as human body at high field. To overcome this problem, RF technologies such as the multi-transmit array coil have been developed along with understanding RF wave behavior inside a dielectric sample. One of important results is that transmission and reception RF fields differ and can be represented as $\mathbf{B}_1^+$ and $\mathbf{B}_1^{-*}$, respectively, where these are complex vectors and * denotes complex conjugate (1). We cannot measure B_1^- in the NMR experiments, which is an RF field component travelling in a direction opposite to nuclear spin precession. Collins graphically demonstrated the proportionality of the reception field to B_1^- in the experiments and simulations of a saline phantom at 7 T, where the similarity was shown between the magnitude image measured by the gradient echo sequence and the calculated image with computed $||\mathbf{B}_1^+||$ and $||\mathbf{B}_1^{-*}||$ (2). Recently, Wang proposed the rotating object method where $||\mathbf{B}_1^-||$ can be measured by the inverted static magnetic field B_0 (3). In this work, we demonstrate the proportionality of the reception filed to $\mathbf{B}_1^{-*}$ straightforwardly in NMR experiments at 4.7 T where the reception field and $||\mathbf{B}_1^{-*}||$ are measured by this method and distribution patterns of magnitude and phase are examined.

Method

Figure 1a shows a schematic of a sample inside an RF coil to explain the rotating object method. $\mathbf{B}_1^+$ and $\mathbf{B}_1^-$ denote the RF field components in the rotating frame. In the original configuration where the object of the sample with the RF coil is set at B_0 parallel to the z-axis (Fig. 1b), $\mathbf{B}_1^+$ is utilized as the transmission field component. When B_0 is oriented antiparallel to the z-axis in the inverted configuration, the direction of the transmission field is also inverted and $\mathbf{B}_1^-$ is utilized as the transmission field component (Fig. 1c). Then, $\mathbf{B}_1^-$ is measurable by the experiments.

We performed phantom experiments using a 4.7 T whole-body NMR spectrometer (*INOVA*, Agilent) with a single-channel ("linear") volume TEM coil both for transmission and reception with 300-mm diameter. A 130-mm diameter spherical saline phantom doped with copper sulfate was set in the RF coil. Transmission field maps were measured by the phase method (4) where a phase of NMR signal depends only on amplitude of the RF field. For reception field mapping, images were obtained by an adiabatic spin echo (ASE) sequence. In this sequence, SE signals were refocused by a $\pi/2$ adiabatic half-passage pulse without slice selection followed by a pair of hyperbolic secant pulses along with slice gradients for a 2D slice selection of 2.5-mm thickness. The magnitude of this ASE image obtained with homogeneous excitation was considered as the reception field map. Next, after the object was rotated 180 degrees around the vertical axis (i. e., the y-axis in Fig. 1) to achieve the inverted configuration, both maps of transmission and reception fields were also measured. In the both configurations, phase maps of the ASE images were also measured. It should be noted that the obtained images must be flipped horizontally when the inverted configuration is achieved by rotating the object.

Results & Discussion

Magnitude distributions

In both of the original and inverted configurations, maps of transmission and reception fields differ in distribution and show mirror symmetry about the axis which passes through the feeding port on the RF coil. The reception field map in the original configuration has almost the same distribution pattern as the transmission field map in the inverted configuration. This result shows the proportionality of reception field to $||\mathbf{B}_1^-||$ in magnitude.

Phase distributions

The phase of the ASE image consists of the two kinds of phases; the phase of transmission field by the $\pi/2$ pulse and that of the reception field. When $\mathbf{B}_{1\text{reception}}$ is parallel to the complex conjugate of $\mathbf{B}_1^-$, the phases in the original and inverted configurations should be $(\phi^+ - \phi^-)$ and $-(\phi^- - \phi^+) = (\phi^+ - \phi^-)$, respectively, where $\mathbf{B}_{1\text{reception}}$, ϕ^+ and ϕ^- denote the reception field and the phases of $\mathbf{B}_1^+$ and $\mathbf{B}_1^-$, respectively. Then, the phases in the both configurations should be the same. It should be noted that the direction of the phase in the inverted configuration is opposite to that in the original one (see Fig. 1b,c). When $\mathbf{B}_{1\text{reception}}$ is parallel to $\mathbf{B}_1^-$, those phases should be $(\phi^+ + \phi^-)$ and $-(\phi^- + \phi^+)$, respectively and the signs of those phases should be opposite. In the measurements, we obtained almost the same phase patterns in the original and inverted configurations (Fig. 3). This result shows that the reception field is parallel to $\mathbf{B}_1^{-*}$. Then, we conclude that the reception field is proportional to $\mathbf{B}_1^{-*}$ in a complex vector space.

References

1. Hoult, D. I., *Concepts Magn. Reson.* 12, 173-183, 2000., 2. Collins, C.M., Yang, Q.X., Wang, J. H., Zhang, X., Michaeli, H., Zhu, X.-H., Adriany, G., Vaughan, J. T., Anderson, P., Merkle, H., Uğurbil, K., Smith, M. B., Chen, W., Magn. Reson. Med., 47, 1026-1028, 2002, 3. Wang, J., Watzl, J., de Graaf, R., Constable, T., *Proc. Intl, Soc. Mag. Reson. Med.*, 17, 4564, 2009., 4. Park, J. Y., Garwood, M., *Proc. Intl, Soc. Mag. Reson. Med.*, 16, 361, 2008.

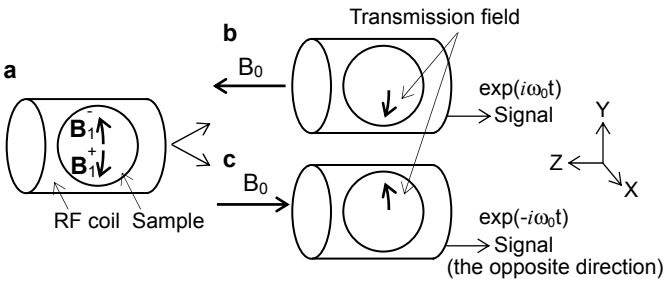

Fig. 1. A schematic of the rotating object method. The case of the inverted B_0 is shown; the original (b) and the inverted (c) configurations.

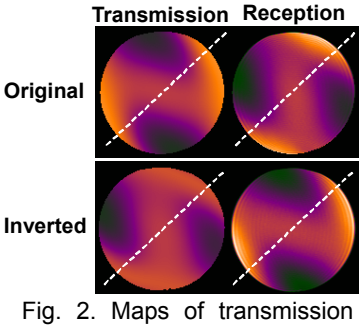

Fig. 2. Maps of transmission and reception fields of a saline phantom. The axis which passes through the feeding port in the RF coil are shown as the white broken lines.

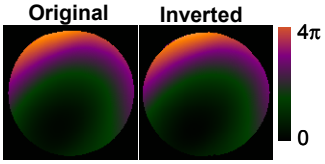

Fig. 3. Phase maps of the ASE images.